

# The role of $N^*(1535)$ in $\eta'$ production

Xu Cao<sup>1,3\*</sup>, Xi-Guo Lee<sup>1,2†</sup>

1. *Institute of Modern Physics, Chinese Academy of Sciences,*

*P.O. Box 31, Lanzhou 730000, P.R.China*

2. *Center of Theoretical Nuclear Physics,*

*National Laboratory of Heavy Ion Collisions, Lanzhou 730000, P.R.China*

3. *Graduate School, Chinese Academy of Sciences, Beijing 100049, P.R.China*

## Abstract

We study the near-threshold  $\eta'$  production mechanism in nucleon-nucleon and  $\pi N$  collisions under the assumption that sub-threshold resonance  $N^*(1535)$  is predominant. In an effective Lagrangian approach which gives a reasonable description to the  $pN \rightarrow pN\eta$  and  $\pi p \rightarrow p\eta$  reactions, it is found that t-channel  $\pi$  exchange make the dominate contribution to the  $pN \rightarrow pN\eta'$  process, and a value of 6.5 for the ratio of  $\sigma(pn \rightarrow pn\eta')$  to  $\sigma(pp \rightarrow pp\eta')$  is predicted. A strong coupling strength of  $N^*(1535)$  to  $\eta'N$  ( $g_{\eta'NN^*}^2/4\pi = 1.1$ ) is extracted from a combined analysis to  $pp \rightarrow pp\eta'$  and  $\pi N \rightarrow N\eta'$ , and the possible implication to the intrinsic component of  $N^*(1535)$  is explored.

PACS numbers: 13.75.-n, 13.75.Cs, 14.20.Gk

---

\* Email: caoxu@impcas.ac.cn

† Email: xgl@impcas.ac.cn

## I. INTRODUCTION

As the members of the nonet of the lightest pseudoscalar mesons, the  $\eta$  and  $\eta'$  mesons have been the subject of considerable interest since accurate and complete measurements have been performed at the experimental facilities of COSY, MAMI, DISTO, GRAAL, CELSIUS and SATURNE in the past few years. Their intrinsic structure and properties, as well as the production mechanism in elementary particle and hadron physics, are intensively explored. The physically observed  $\eta$  and  $\eta'$  mesons are mixtures of the pseudoscalar octet and singlet, which results in a considerable amount of  $s\bar{s}$  in both and accounts for the difference in  $\eta$  mass from the pion. The much greater mass of  $\eta'$  meson is thought to be induced by the non-perturbative gluon dynamics[1] and the axial anomaly[2].

The  $\eta$  and  $\eta'$  production in nucleon-nucleon collisions strengthen our understanding on those problems and also provide assistant opportunities to study the possible nucleon resonances  $N^*$  that couple only weakly to pion. Due to the precise measurements of the total cross section of the  $pp \rightarrow pp\eta$  reaction[3, 4, 5, 6, 7], a number of studies[8, 9, 10, 11, 12, 13, 14, 15, 16] have concluded that  $\eta$  meson is dominantly produced through the excitation and de-excitation of the  $N^*(1535)$  resonance in this reaction, though the excitation mechanism is still under debate. The first measurement of the cross section of the quasi-free  $pn \rightarrow pn\eta$  reaction[17] shows about a factor of 6.5 larger than that of  $pp \rightarrow pp\eta$ , clearly indicating a dominance of isovector exchange. A recent experimental study of the analyzing power of the  $\vec{p}p \rightarrow pp\eta$  reaction[18] support that the  $\pi$  meson exchange between the colliding nucleons is predominant. On the other hand, for the lack of experimentally established baryonic resonances which would decay into  $\eta'$ , our understanding of the  $\eta'$  production is still much poorer and unsatisfactory, and there are only a limited number of studies both experimentally[4, 19, 20, 21, 22] and theoretically[23, 24, 25, 26]. An early analysis based on the covariant one Boson exchange(OBE) model[24] reproduces the near-threshold total cross section of the  $pp \rightarrow pp\eta'$  reaction without any resonant term. However, a relativistic meson exchange model[25] demonstrates that the existing data could be explained either by mesonic and nucleonic currents or by a dominance of two missing resonances  $S_{11}(1897)$  and  $P_{11}(1986)$ . The extended study[26] motivated by the updated data of the  $\gamma p \rightarrow \eta' p$ [20] and  $pp \rightarrow pp\eta'$ [21, 22] yields resonances  $S_{11}(1650)$  and  $P_{11}(1870)$ , and it is premature to identify these states, as these authors pointed out. Besides, another compli-

cation comes from the gluon-induced contact term[27], which would have extra contribution to the cross-section for  $pp \rightarrow pp\eta'$ , since it is possible that  $\eta'$  meson couples strongly to gluons.

Recently, high-precision data of the reaction  $\gamma p \rightarrow \eta' p$  for photon energies from 1.527GeV to 2.227GeV are obtained by the CLAS Collaboration[28], and the analysis[28, 29] of these data suggest for the first time that both the  $N^*(1535)$  and  $N^*(1710)$  resonances, known to couple strongly to the  $\eta N$  channel, couple to the  $\eta' N$  channel. This is obviously the evidence for the important role of these resonances in the  $\eta'$  production. Theoretically,  $N^*(1535)$  is found to be important for the near-threshold  $\Lambda$  and  $\phi$  production in nucleon-nucleon collisions[30], and a significant coupling of  $N^*(1535)$  to strange particles is indicated. Furthermore, the properties of  $N^*(1535)$  resonance are extensively discussed in chiral unitary approach[31], and large couplings to  $\eta N$ ,  $K\Sigma$  and  $K\Lambda$  are also illustrated.

Motivated by these research, in this paper we assume that the excitation and de-excitation of the  $N^*(1535)$  resonance play a major role in the  $\eta'$  production in the near-threshold region, and perform a consistent analysis to the reactions  $pp \rightarrow pp\eta(\eta')$ ,  $pn \rightarrow pn\eta(\eta')$  and  $\pi N \rightarrow N\eta(\eta')$  in the framework of an effective lagrangian approach. Because the coupling strength of  $\eta'$  meson to the nucleon and  $N^*$  are poorly known[26, 28, 29], in our analysis we do not include  $N^*(1650)$  and  $N^*(1710)$ , which are expected to have very small contribution to the considered energy region[15]. The inclusion of the nucleonic and mesonic currents in the intermediate state is found to make negligible difference in the final results[12, 15], so we do not consider them either.

## II. EFFECTIVE LAGRANGIAN APPROACH

We treat the reactions  $pp \rightarrow pp\eta(\eta')$  and  $\pi N \rightarrow N\eta(\eta')$  at the relativistic tree level in an effective Lagrangian approach, as depicted by Feynman diagrams in Fig. 1. Mesons exchanged are restricted to those observed in the decay channels of the adopted resonances, and most values of the coupling constants are fixed by the experimental decay ratios. As a result, the only adjustable parameters are cut-off parameters in the form factors. All interference terms between different amplitudes are neglected because the relative phases of these amplitudes are not known. The relevant meson-nucleon-nucleon(MNN) and meson-nucleon-resonance(MNR) effective Lagrangians for evaluating the Feynman diagrams in Fig.

1 are[30, 32]:

$$L_{\pi NN} = -ig_{\pi NN}\bar{N}\gamma_5\vec{\tau} \cdot \vec{\pi}N, \quad (1)$$

$$L_{\rho NN} = -g_{\rho NN}\bar{N}(\gamma_\mu + \frac{\kappa}{2m_N}\sigma_{\mu\nu}\partial^\nu)\vec{\tau} \cdot \vec{\rho}N, \quad (2)$$

$$L_{\eta NN} = -ig_{\eta NN}\bar{N}\gamma_5N\eta, \quad (3)$$

$$L_{\pi NN^*} = -g_{\pi NN^*}\bar{N}^*\gamma_5\vec{\tau} \cdot \vec{\pi}N^* + h.c., \quad (4)$$

$$L_{\rho NN^*} = ig_{\rho NN^*}\bar{N}^*\gamma_5(\gamma_\mu - \frac{q_\mu\gamma \cdot q}{q^2})\vec{\tau} \cdot \vec{\rho}N^* + h.c., \quad (5)$$

$$L_{\eta NN^*} = -g_{\eta NN^*}\bar{N}^*N^*\eta + h.c., \quad (6)$$

$$L_{\eta' NN^*} = -g_{\eta' NN^*}\bar{N}^*N^*\eta' + h.c. \quad (7)$$

with  $g_{\pi NN}^2/4\pi = 14.4$ ,  $g_{\rho NN}^2/4\pi = 0.9$ , and  $\kappa = 6.1$ . The coupling constant  $g_{\eta NN}$  is undetermined nowadays, and the value of  $g_{\eta NN}^2/4\pi$  used in literature is ranging from 0.25 to 7[33]. Recent calculations[9, 10, 13, 14, 30] seem to favor small  $g_{\eta NN}$ , and  $g_{\eta NN}^2/4\pi = 0.4$ [30] are used in our calculation. The partial decay width of  $N^*(1535) \rightarrow N\pi$ ,  $N^*(1535) \rightarrow N\rho \rightarrow N\pi\pi$  and  $N^*(1535) \rightarrow N\eta$  then can be calculated by above Lagrangians, and the coupling constants  $g_{\pi NN^*}^2/4\pi$ ,  $g_{\rho NN^*}^2/4\pi$ , and  $g_{\eta NN^*}^2/4\pi$  are determined through the empirical branching ratios[30, 32], as summarized in Table I. Up to now, we have no information on the coupling constant of the  $\eta' NN^*(1535)$  vertex, and we determine it from a combined analysis of  $pp \rightarrow pp\eta'$  and  $\pi N \rightarrow N\eta'$  reactions.

In order to dampen out high values of the exchanged momentum, the resulting vertexes are multiplied by off-shell form factors. In  $pp \rightarrow pp\eta(\eta')$  reactions, the form factors used in the Bonn model[33] are taken:

$$F_M(q^2) = \left( \frac{\Lambda_M^2 - m_M^2}{\Lambda_M^2 - q_M^2} \right)^n, \quad (8)$$

with  $\Lambda_M$ ,  $q_M$  and  $m_M$  being the cut-off parameter, four-momentum and mass of the exchanged meson. The commonly used  $n = 2$  for  $\rho NN$  vertex, and  $n = 1$  for other vertexes, are employed. The cut-off parameters  $\Lambda_\pi = 1.05\text{GeV}$  for  $\pi NN$ ,  $\Lambda_\rho = 0.92\text{GeV}$  for  $\rho NN$ ,  $\Lambda_\eta = 2.00\text{GeV}$  for  $\eta NN$  and  $\Lambda_M = 0.80\text{GeV}$  for MNR vertexes are adopted from Ref.[32], which performed a systematic consistent investigation of the strangeness production process in nucleon-nucleon collisions. In  $\pi N \rightarrow N\eta(\eta')$  reactions, the following form factors for  $N^*(1535)$  resonance are used[25, 26, 29, 30]:

$$F_{N^*}(q^2) = \frac{\Lambda^4}{\Lambda^4 + (q^2 - M_{N^*}^2)^2}, \quad (9)$$

with the cut-off parameter  $\Lambda = 2\text{GeV}$ .

Propagators of  $\pi(\eta)$ ,  $\rho$  and  $N^*(1535)$  are:

$$G_M(q_M) = \frac{i}{q_M^2 - m_M^2}, \quad (10)$$

$$G_\rho^{\mu\nu}(q_\rho) = -i \frac{g^{\mu\nu} - q_\rho^\mu q_\rho^\nu / q_\rho^2}{q_\rho^2 - m_\rho^2}, \quad (11)$$

$$G_R(p_R) = \frac{\gamma \cdot p_R + m_R}{p_R^2 - m_R^2 + im_R \Gamma_R}. \quad (12)$$

With above formalism, the invariant amplitude can be obtained straightforwardly by applying the Feynman rules to Fig. 1.

It is generally agreed that  $^1S_0$  proton-proton final state interaction (FSI) influences the near-threshold behavior significantly in  $pp \rightarrow pp\eta(\eta')$ . In present calculation, Watson-Migdal factorization[34] are used and the pp FSI enhancement factor is taken to be Jost function[35]:

$$|J(k)|^{-1} = \frac{k + i\beta}{k - i\alpha}. \quad (13)$$

where  $k$  is the internal momentum of  $pp$  subsystem. The related scattering length and effective range are:

$$a = \frac{\alpha + \beta}{\alpha\beta}, \quad r = \frac{2}{\alpha + \beta}, \quad (14)$$

with  $a = -7.82\text{fm}$  and  $r = 2.79\text{fm}$ (i.e.  $\alpha = -20.5\text{MeV}$  and  $\beta = 166.7\text{MeV}$ ) for  $^1S_0$   $pp$  interaction.

Then the total cross section can be calculated by above prescription, and the integration over the phase space can be performed by Monte Carlo program. As to the  $pn \rightarrow pn\eta(\eta')$  reaction, isospin factors are considered[9, 11, 15], and  $a = -23.76\text{fm}$  and  $r = 2.75\text{fm}$ (i.e.  $\alpha = -7.87\text{MeV}$  and  $\beta = 151.4\text{MeV}$ ) for  $^1S_0$   $pn$  interaction,  $a = 5.424\text{fm}$  and  $r = 1.759\text{fm}$ (i.e.  $\alpha = 45.7\text{MeV}$  and  $\beta = 178.7\text{MeV}$ ) for  $^3S_1$   $pn$  interaction are used.

### III. NUMERICAL RESULTS

We first apply our approach to the  $\eta$  production, and check the applicability of our model. Total cross section for  $pp \rightarrow pp\eta$ ,  $\pi^- p \rightarrow n\eta$  and  $pn \rightarrow pn\eta$  are shown in Fig. 2, and our numerical results agree well with the experimental data. Contributions of various meson exchanges to  $pp \rightarrow pp\eta$  and  $pn \rightarrow pn\eta$  are also shown, and  $\pi$  exchange is found

to make dominant contribution in the near-threshold region. This has received support from recent experiment[18], and also the reason for our simultaneous reproduce to these two channels[11, 15, 17]. In sharp contrast to Ref.[9] which indicates  $\rho$  exchange dominance, the contribution of  $\rho$  exchange is much smaller than that of  $\pi$  and  $\eta$  exchange in our calculation. Besides, in a calculation[30] to  $pp \rightarrow pp\phi$  reaction whose approach is similar to us, it is demonstrated that the contribution of  $\rho$  exchange is larger than that of  $\eta$  exchange though  $\pi$  exchange is dominant in the  $N^*(1535)$  excitation. This difference to our model is caused by the alternative cut-off parameters in the form factors, and much larger values( $\Lambda = 1.6GeV$  for  $\rho NN$  vertex and  $\Lambda = 1.3GeV$  for all other form factors) are used in their model. It seems that the vector couplings of the  $\rho NN$  vertex are suppressed more fast than the pseudo-scalar couplings of  $\pi NN$  and  $\eta NN$  vertex when the cut-off parameters are decreased. In the considered energy region, the small cut-off parameters should be more reasonable, as already illustrated in the analysis to the strangeness production process in nucleon-nucleon collisions[32]. Similarly, our model should draw some analogous conclusions to the  $pN \rightarrow pN\eta'$  channel in this aspect due to the formalism of our model, as demonstrated below. The relatively larger  $\eta$  exchange contribution than that of  $\rho$  exchange is also found in Refs.[11, 14], but it is worth pointing out that a very small  $g_{\eta NN}$  is adopted in our model.

As can be seen from Fig. 2(a)(c), there is no much room left to the coherent resonance-resonance interference term, which is thought to be non-negligible, as stressed in Ref.[15]. The cross section of  $\pi^-p \rightarrow n\eta$  where  $T_\pi > 850MeV$  is underestimated as displayed in Fig. 2(b), and this is obviously the evidence to the contribution of other resonances(i.e.  $N^*(1650)$  and  $N^*(1710)$ ) in this energy region.

For excess energies smaller than 20MeV, theoretical results underestimate the empirical cross section of  $pp \rightarrow pp\eta$  channel, as several authors pointed out[11, 15]. The discrepancy in invariant mass distribution is even more pronounced, as can be clearly seen in Fig. 3(a-d). In addition to a peak arising from the  $N^*(1535)$  resonance and strong  $^1S_0$  pp FSI, there is a surprising broad bump in both  $pp$  and  $p\eta$  invariant mass distribution, which is not trivial to be explained. Some papers devote to this problem, and the origin of the bump is attributed to the large  $\eta$  meson exchange contribution comparable with the leading  $\pi$  meson exchange term[14] or higher partial waves[12]. However, former hypothesis apparently conflicts with the experimental finding of a dominance of isovector exchange, thus it can not account for the high ratio of  $\sigma(pn \rightarrow pn\eta)$  to  $\sigma(pp \rightarrow pp\eta)$ . The latter can not give simultaneous explanation

of the excitation function and invariant mass distributions, and the visible bump at excess energies of 4.5MeV[7] is either improbably caused by the contribution of higher partial waves. As a result, it seems that this bump probably arises from the  $\eta N$  FSI[16]. Unfortunately, till now there is no rigorous treatment of three-pair FSI, and this problem needs further theoretical and experimental effort. As shown in Fig. 3(e-f), the angular distribution of  $\eta$  meson in the  $pp \rightarrow pp\eta$  reaction for excess energies of 15MeV and 41MeV are described well by our model, since our model is characterized by the  $\pi$  exchange dominance process in the  $N^*(1535)$  excitation.

Then we will employ our model to  $\eta'$  production since its success to  $\eta$  production has been demonstrated above. Total cross section for  $pp \rightarrow pp\eta'$ ,  $\pi N \rightarrow N\eta'$  and  $pn \rightarrow pn\eta'$  are shown in Fig. 4. We get good reproduce to both  $pp \rightarrow pp\eta'$  and  $\pi N \rightarrow N\eta'$  channels with  $g_{\eta'NN^*}^2/4\pi = 1.1$ , and some similar conclusions to  $\eta$  production are achieved as expected.  $\pi$  exchange is the largest contribution in the near-threshold region of  $pN \rightarrow pN\eta'$ , and  $\rho$  exchange is much smaller than  $\pi$  and  $\eta$  exchange. Without complexity caused by  $\eta'N$  interaction[19, 23], our numerical results reproduce the experimental data quite well in the whole considered energy region. As can be seen in Fig. 4(c), we anticipate the same value of 6.5 for the ratio of  $\sigma(pn \rightarrow pn\eta')$  to  $\sigma(pp \rightarrow pp\eta')$  in our model, while this ratio will approach unity if  $\eta'$  is produced directly by gluons[27]. So isospin dependence is powerful to distinguish different  $\eta'$  production mechanism, and may provide useful information to the possible gluon content of  $\eta'$  meson.

For the scarce and inaccurate data of  $\pi N \rightarrow N\eta'$ , the extracted coupling constant  $g_{\eta'NN^*}$  has large err bar, and significant contributions from other  $N^*$  resonances cannot be definitely excluded. Alternative combination of  $N^*$  resonances and coupling strength would yield a good fit to present data[30]. The dotted curve in Fig. 4(b) shows that we can get a much better reproduce to the  $\pi N \rightarrow N\eta'$  data with  $g_{\eta'NN^*}^2/4\pi = 1.0$ , although this will slightly underestimate the  $pp \rightarrow pp\eta'$  channel. An even better fit to the  $pp \rightarrow pp\eta'$  data can be achieved with  $g_{\eta'NN^*}^2/4\pi = 1.15$ , but this will overestimate the  $\pi N \rightarrow N\eta'$  data as shown by the dashed line in Fig 4(b). Anyway, we get good result to both channels with  $g_{\eta'NN^*}^2/4\pi = 1.1$ , and our preliminary analysis should be reasonable considering that other  $N^*$  resonances except  $N^*(1535)$  show very weak couplings to  $\eta'N$ .

The calculated invariant mass spectrum of  $pp \rightarrow pp\eta'$  reaction at the excess energies of 15.5MeV, 46.6MeV and 143.8MeV are presented in Fig. 5. Our calculations of angular

distribution of  $\eta'$  meson at 46.6MeV and 143.8MeV show obvious structure at forward and backward angles, and reproduce the experimental data nicely. However, it has to admitted that the measured angular dependence might be also compatible to isotropic shape within the given experimental uncertainties. Besides, it is interesting to note that the data from Ref.[5] show distinct structure in the angular distribution of  $\eta$  meson, but Ref.[6] gives a totally flat distribution, as can be seen in Fig. 3(e-f). So a detailed quantitative analysis awaits for the clearing of the experimental situation.

The predicted differential cross section of  $pp \rightarrow pp\eta'$  at the excess energy of 15.5MeV, together with the total cross section of  $pn \rightarrow pn\eta'$ , can be examined by the ongoing experimental studies[16]. No obvious bump other than a peak arise in the invariant mass distribution because our model do not include additional mechanism rather than the  $N^*(1535)$  resonance and FSI. If this is confirmed by the experiment, then other mechanism(probably the  $\eta N$  FSI) accounting for the broad bump should be added to the study of the  $pp \rightarrow pp\eta$  channel.

#### IV. SUMMARY AND DISCUSSION

In this paper, we present a consistent analysis to  $pN \rightarrow pN\eta'$  and  $\pi N \rightarrow N\eta'$  within an effective Lagrangian approach, assuming that  $N^*(1535)$  resonance is dominant in the  $\eta'$  production. Our numerical results show that  $\pi$  exchange is the most important in  $pN \rightarrow pN\eta'$  reaction, and predict a large ratio of  $\sigma(pn \rightarrow pn\eta')$  to  $\sigma(pp \rightarrow pp\eta')$ . An explicit structure in angular distribution of  $\eta'$  meson is demonstrated. Besides, a significant coupling strength of  $N^*(1535)$  to  $\eta'N$  is found:

$$g_{\eta'NN^*}^2/4\pi = 1.1 \quad (15)$$

In a vector-meson-dominant model analysis to  $\gamma p \rightarrow p\eta'$  reaction[37], a value of  $g_{\eta'NN^*} = 3.4$ (i.e.  $g_{\eta'NN^*}^2/4\pi = 0.92$ ) is given, and this is coincident to our analysis. We would illustrate that this is also compatible to the mixture picture of  $\eta$  and  $\eta'$ .

Considering the possible gluonium admixture of the  $\eta'$  wave function, a basis of states  $|\eta_q\rangle = |u\bar{u} + d\bar{d}\rangle/\sqrt{2}$ ,  $|\eta_s\rangle = |s\bar{s}\rangle$  and  $|G\rangle = |Gluonium\rangle$  is adopted, and the physical  $\eta$  and  $\eta'$  are assumed to be linear combinations of these basis of states[38, 39]:

$$|\eta\rangle = X_\eta|\eta_q\rangle + Y_\eta|\eta_s\rangle + Z_\eta|G\rangle \quad (16)$$



$$|\eta'\rangle = X_{\eta'}|\eta_q\rangle + Y_{\eta'}|\eta_s\rangle + Z_{\eta'}|G\rangle \quad (17)$$

If the gluonium content of the  $\eta$  meson is assumed to vanish ( $Z_\eta = 0$ ), all six parameters can be written in terms of two mixing angles,  $\phi_p$  and  $\phi_{\eta'G}$ , which correspond to:

$$X_\eta = \cos\phi_p, \quad Y_\eta = -\sin\phi_p, \quad Z_\eta = 0, \quad (18)$$

$$X_{\eta'} = \sin\phi_p \cos\phi_{\eta'G}, \quad Y_{\eta'} = \cos\phi_p \cos\phi_{\eta'G}, \quad Z_{\eta'} = -\sin\phi_{\eta'G}. \quad (19)$$

If the gluonium content of the  $\eta'$  meson is further assumed to vanish ( $Z_{\eta'} = 0$ , i.e.  $\phi_{\eta'G} = 0$ ), then  $\phi_p$  is the  $\eta - \eta'$  mixing angle in absence of gluonium, and Eqs.(16)(17) are the normal  $\eta - \eta'$  mixing in the quark-flavor basis. In the quark model, the  $\eta'$  couplings can be related to those of  $\eta$ [24, 37]:

$$g_\eta = X_\eta g_q + Y_\eta g_s + Z_\eta g_G \quad (20)$$

$$g_{\eta'} = X_{\eta'} g_q + Y_{\eta'} g_s + Z_{\eta'} g_G \quad (21)$$

with  $g_q$ ,  $g_s$  and  $g_G$  being the non-strangeness, strangeness and gluonium coupling constant. As to  $g_{\eta'NN}$  and  $g_{\eta NN}$ , because the strangeness and gluonium content in nucleon are negligible, we can take the simplifying assumption  $g_s \ll g_q$  and  $g_G \ll g_q$ :

$$R_N = \frac{g_{\eta'NN}}{g_{\eta NN}} \simeq \frac{X_{\eta'}}{X_\eta} = \tan\phi_p \sim 0.84 \quad (22)$$

with  $\phi_p \sim 40^\circ$ [40]. This is compatible to  $R_N \sim 0.62$  with recently extracted value of  $g_{\eta'NN} \simeq 1.4$ [28] and adopted  $g_{\eta NN}^2/4\pi = 0.4$  in this paper.

With coupling constants summarized in Table. I, we have:

$$R_{N^*} = \frac{g_{\eta'NN^*}}{g_{\eta NN^*}} \sim 2.0 \quad (23)$$

If the large  $g_{\eta'NN^*}$  indeed indicates a significant  $s\bar{s}$  configuration inside  $N^*(1535)$  resonance[30], assuming  $g_{GNN^*} \ll g_{qNN^*}$  should be reasonable:

$$R_{N^*} = \frac{g_{\eta'NN^*}}{g_{\eta NN^*}} = \frac{\tan\phi_p + g_{sNN^*}/g_{qNN^*}}{1 - g_{sNN^*}/g_{qNN^*}\tan\phi_p} \quad (24)$$

Then we will get  $g_{sNN^*}/g_{qNN^*} \sim 0.43$ , which may indicate a relatively large proportion of strangeness in  $N^*(1535)$  resonance. But the large  $g_{\eta'NN^*}$  is also probably caused by the gluonium component of  $N^*(1535)$  as can be seen in Eqs.(20)(21), then if  $g_{sNN^*} \ll g_{qNN^*}$  is assumed:

$$R_{N^*} = \frac{g_{\eta'NN^*}}{g_{\eta NN^*}} = \tan\phi_p \cos\phi_{\eta'G} - \frac{g_{GNN^*}}{g_{qNN^*}} \frac{\sin\phi_{\eta'G}}{\cos\phi_p} \quad (25)$$

where  $\phi_p \sim 40^\circ$  and  $|\phi_{\eta'G}| \sim 22^\circ$ [38]. Then we will get  $|g_{GNN^*}/g_{qNN^*}| \sim 2.5$ , and this may also indicate a relatively large proportion of gluons in  $N^*(1535)$  resonance. Certainly, according to above analysis, it is possible that strangeness and gluons coexist in  $N^*(1535)$ , and it is two of them that induce the large couplings of  $N^*(1535)$  to strange particles. Recently, phenomenological analysis of radiative decays and other processes[39] conclude no evidence of the gluonium contribution of  $\eta'$  wave function(i.e.  $|\phi_{\eta'G}| \sim 0^\circ$ ), and this seems to support the idea that these large couplings are major caused by the  $s\bar{s}$  component in  $N^*(1535)$ . Different 5-quark configurations of  $qqqs\bar{s}$  have deeply investigated, and admixture of 25-65% in  $N^*(1535)$  is suggested[41]. However, the intrinsic structure of  $N^*(1535)$  is still left to be an open question and further study are needed.

In conclusion, our phenomenological analysis to the  $\eta'$  production in nucleon-nucleon and  $\pi N$  collisions not only give nice reproduce to the experimental data, but also agree well with the present understanding of the internal component of the  $\eta$  ( $\eta'$ ) meson and  $N^*(1535)$  resonance, although alternative contribution from other  $N^*$  resonances are also possible. The ongoing relevant experiment in COSY[16] will soon examine our results and advance a better knowledge of the  $\eta$  and  $\eta'$  production.

### Acknowledgments

We would like to thank Q. W. Wang, J. J. Xie and B. S. Zou for fruitful discussions and program code. This work was supported by the CAS Knowledge Innovation Project (No.KJ CX3-SYW-N2, No.KJ CX2-SW-N16) and Science Foundation of China (10435080, 10575123, 10710172).

- 
- [1] G. 't Hooft, *Phys. Rev. Lett.* **37**, 8 (1976); E. Witten, *Nucl. Phys. B* **156**, 269 (1979).
  - [2] S. L. Adler, *Phys. Rev.* **177**, 2426 (1969).
  - [3] J. Smyrski et al., *Phys. Lett. B* **474**, 182 (2000); H. Calen et al., *ibid.* **366**, 39 (1996); E. Chiavassa et al., *ibid.* **322**, 270 (1994); A. M. Bergdolt et al., *Phys. Rev. D* **48**, R2969 (1993); F. Balestra et al., *Phys. Rev. C* **69**, 064003 (2004).
  - [4] F. Hibou et al., *Phys. Lett. B* **438**, 41 (1998).
  - [5] H. Calen et al., *Phys. Lett. B* **458**, 190 (1999).

- [6] M. Abdel-Bary et al., *Eur. Phys. J. A* **16**, 127 (2003).
- [7] P. Moskal et al., *Phys. Rev. C* **69**, 025203 (2004).
- [8] J. M. Laget et al., *Phys. Lett. B* **257**, 254 (1991); T. Vetter et al., *ibid.* **263**, 153 (1991); M. Batinić et al., *Physica. Scripta.* **56**, 321 (1997); E. Gedalin et al., *Nucl. Phys. A* **650**, 471 (1999); V. Bernard et al., *Eur. Phys. J. A* **4**, 259 (1999).
- [9] G. Fäldt, and C. Wilkin, *Physica. Scripta.* **64**, 427 (2001).
- [10] M. T. Peña, H. Garcilazo, and D. O. Riska, *Nucl. Phys. A* **683**, 322 (2001).
- [11] K. Nakayama, J. Speth and T. -S. H. Lee, *Phys. Rev. C* **65**, 045210 (2002).
- [12] K. Nakayama, J. Haidenbauer, C. Hanhart and J. Speth, *Phys. Rev. C* **68**, 045201 (2003).
- [13] V. Baru et al., *Phys. Rev. C* **67**, 024002 (2003).
- [14] S. Ceci, A. Švarc, and B. Zauner, *Physica. Scripta.* **73**, 663 (2006).
- [15] R. Shyam, *Phys. Rev. C* **75**, 055201 (2007).
- [16] P. Moskal et al., *Int. J. Mod. Phys. A* **22**, 305 (2007).
- [17] H. Calen et al., *Phys. Rev. C* **58**, 2667 (1998).
- [18] R. Czyżykiewicz et al., *Phys. Rev. Lett.* **98**, 122003 (2007).
- [19] P. Moskal et al., *Phys. Rev. Lett.* **80**, 3202 (1998); P. Moskal et al., *Phys. Lett. B* **474**, 416 (2000); P. Moskal et al., *ibid* **482**, 356 (2000).
- [20] ABBHHM Collaboration, *Phys. Rev.* **175**, 1669 (1968); *Nucl. Phys. B* **108**, 45 (1976); R. Plötzke et al., *Phys. Lett. B* **444**, 555 (1998); J. Barth et al., *Nucl. Phys. A* **691**, 374c (2001).
- [21] F. Balestra et al., *Phys. Lett. B* **491**, 29 (2000).
- [22] A. Khoukaz et al., *Eur. Phys. J. A* **20**, 345 (2004).
- [23] A. Sibirtsev and W. Cassing, *Eur. Phys. J. A* **2**, 333 (1998); V. Bernard et al., *ibid* **4**, 259 (1999); V. Baru et al., *ibid* **6**, 445 (1999).
- [24] E. Gedalin, A. Moalem, and L. Razdolskaja, *Nucl. Phys. A* **650**, 471 (1999).
- [25] K. Nakayama, H. F. Arellano, J. W. Durso, and J. Speth, *Phys. Rev. C* **61**, 024001 (1999).
- [26] K. Nakayama, and H. Haberzettl, *Phys. Rev. C* **69**, 065212 (2004).
- [27] S. D. Bass, *Phys. Lett. B* **463**, 286 (1999).
- [28] M. Dugger et al., *Phys. Rev. Lett.* **96**, 062001 (2006); *Erratum-ibid.* **96**, 169905 (2006).
- [29] K. Nakayama, and H. Haberzettl, *Phys. Rev. C* **73**, 045211 (2006).
- [30] B. C. Liu, and B. S. Zou, *Phys. Rev. Lett.* **96**, 042002 (2006); J. J. Xie, B. S. Zou, and H.C. Chiang, *Phys. Rev. C* **77**, 015206 (2008).

TABLE I: Relevant  $N^*(1535)$  parameters

	Width	Channel	Branching ratio	Adopted value	$g^2/4\pi$
$N^*(1535)$	150MeV	$\pi N$	0.35-0.55	0.45	0.033
		$\rho N$	$0.02 \pm 0.01$	0.02	0.10
		$\eta N$	0.45-0.60	0.53	0.28
		$\eta' N$	—	—	1.1

- [31] N. Kaiser, T. Waas, and W. Weise, *Nucl. Phys. A* **612**, 297 (1997).
- [32] K. Tsushima, A. Sibirtsev, A.W. Thomas and G. Q. Li, *Phys. Rev. C* **59**, 369 (1999).
- [33] R. Machleidt, K. Holinde, and Ch. Elster, *Phys. Rep.* **149**, 1 (1987).
- [34] K. Watson, *Phys.Rev.* **88**, 1163 (1952);A.B. Migdal, *Sov. Phys. JETP* **1**, 2(1955).
- [35] M. Goldberger, K.M. Watson, *Collision Theory Willey, New York.* (1964).
- [36] A. Baldini, V. Flamino, W. G. Moorhead and D. R. O. Morrison, *Landolt-Bornstein, Numerical Data and Functional Relationships in Science an Technology, vol.12, ed. by H. Schopper, Springer-Verlag(1988), Total Cross Sections of High Energy Particles.*
- [37] A. Sibirtsev, Ch. Elster, S. Krewald, and J. Speth, *arXiv:nucl-th/0303044*.
- [38] E. Kou, *Phys. Rev. D* **63**, 054027 (2001);F. Ambrosino et al., *Phys. Lett. B* **648**, 267 (2007).
- [39] C. E. Thomas, *JHEP* **0710**, 026 (2007);R. Escribano, *arXiv:hep-ph/0712.1814*.
- [40] T. Feldmann and P. Kroll, *Eur. Phys. J. C* **5**, 327 (1998);KLOE Collaboration, *Phys. Lett. B* **541**, 45 (2002).
- [41] B. S. Zou and D. O. Riska, *Phys. Rev. Lett.* **95**, 072001 (2005);C. S. An and B. S. Zou, *arXiv:nucl-th/0802.3996*.

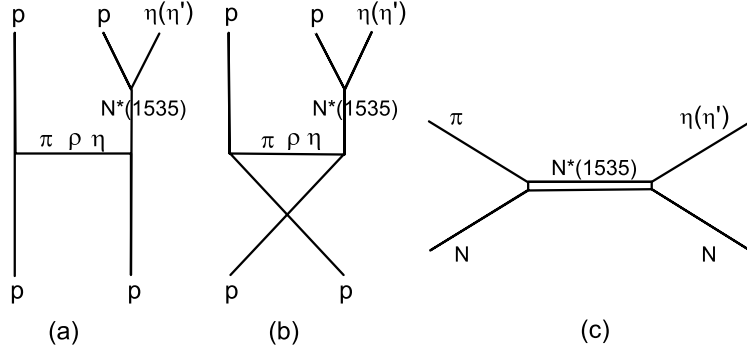


FIG. 1: Feynman diagrams for  $pp \rightarrow pp\eta(\eta')$  and  $\pi N \rightarrow N\eta(\eta')$ .

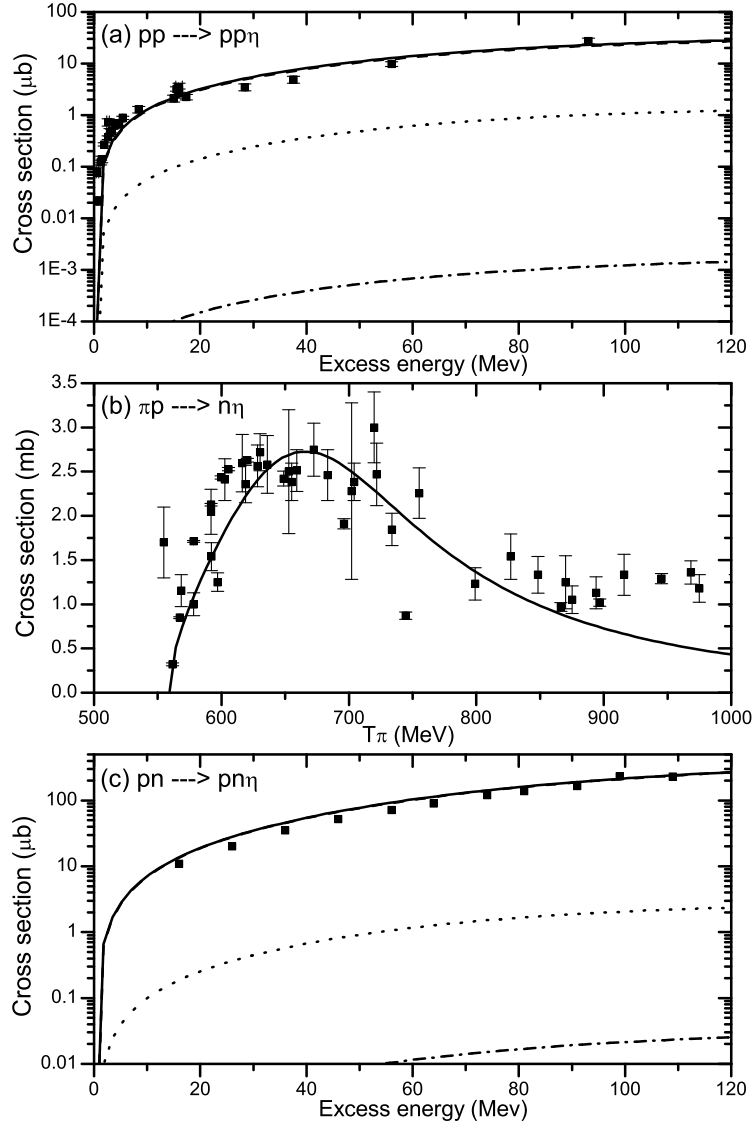


FIG. 2: Total cross section for  $pp \rightarrow pp\eta$ (a),  $\pi^- p \rightarrow n\eta$ (b) and  $pn \rightarrow pn\eta$ (c). (a)(c): The dashed, dotted, dash-dotted and solid curve correspond to contribution from  $\pi$ ,  $\eta$ ,  $\rho$  exchange and their simple sum, respectively. The dashed curve is overlapped by the solid one. The data are from Ref.[3, 4](a), Ref.[36](b) and Ref.[17](c).

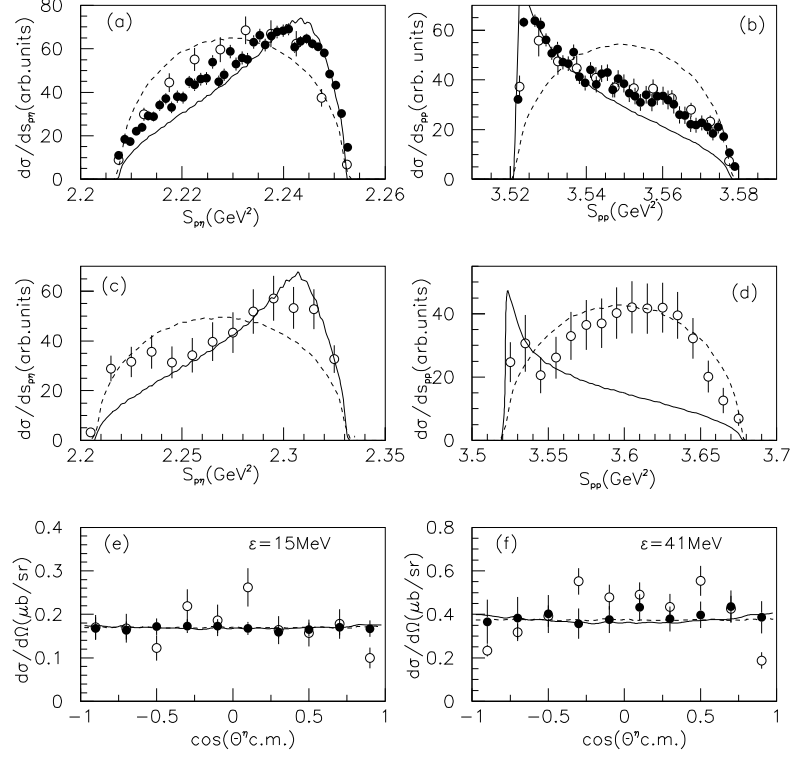


FIG. 3: Invariant mass spectrum for  $pp \rightarrow pp\eta$ . (a)(b)(e) and (c)(d)(f) are invariant mass spectrum at excess energies of 15MeV and 41MeV, respectively. (a-d): The data are from Ref.[6](open circle) and Ref.[7](closed circle). (e-f): The data are from Ref.[5](open circle) and Ref.[6](closed circle). The dashed curve is the pure phase-space distribution.

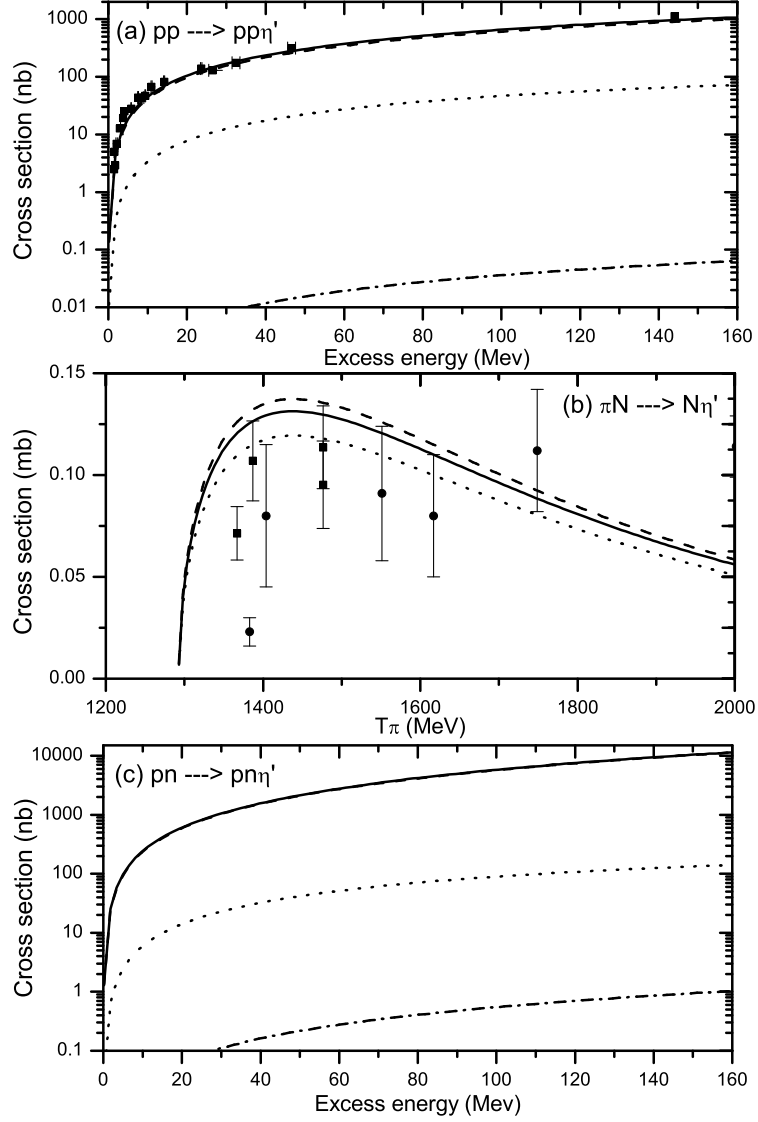


FIG. 4: Total cross section for  $pp \rightarrow pp\eta'$ (a),  $\pi N \rightarrow N\eta'$ (b) and  $pn \rightarrow pn\eta'$ (c). (a)(c): Same as Fig. 2(a)(c). (b): The dashed, solid and dotted curve correspond to  $g_{\eta' NN^*}^2/4\pi = 1.15, 1.1$  and  $1.0$ . The data are from Ref.[19](a), Ref.[36](b)(closed square:  $\pi^- p \rightarrow n\eta'$ , closed circle:  $\pi^+ n \rightarrow p\eta'$ ).



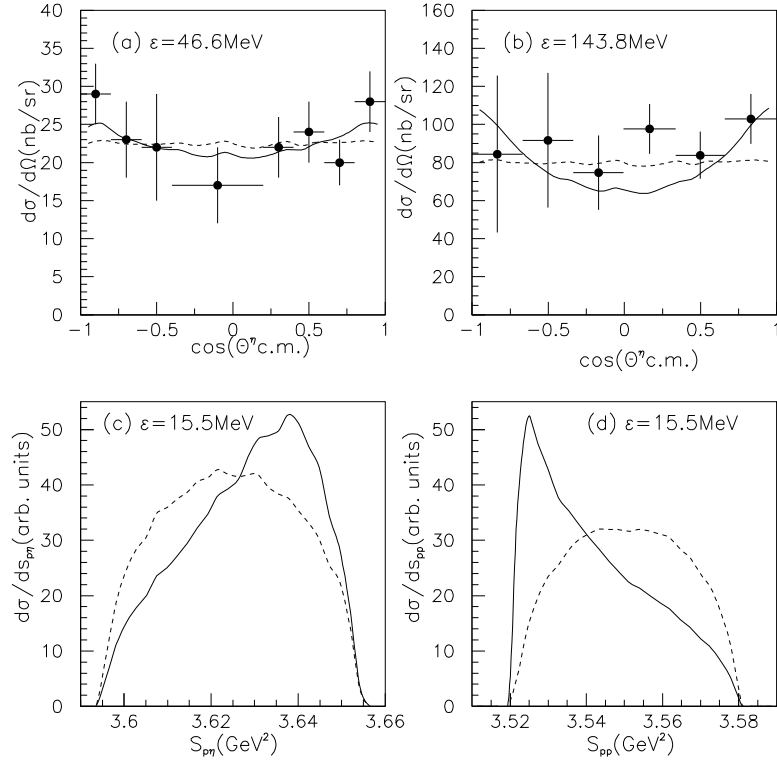


FIG. 5: Invariant mass spectrum for  $pp \rightarrow pp\eta'$ . (a)(b) and (c)(d) are angular distribution of  $\eta$  meson and invariant mass distribution respectively. The data are from Ref.[22](a) and Ref.[21](b). The dashed curve is the pure phase-space distribution.